

Spatial transformation of coherent optical waves with orbital morphologies

Y. F. Chen,* Y. C. Lin, and K. F. Huang

Department of Electrophysics, National Chiao Tung University, 1001 Ta-Hsueh Rd., Hsinchu, 30050, Taiwan

T. H. Lu

Department of Physics, National Taiwan Normal University, 88 Sec. 4 Ting-Chou Rd., Taipei, 116, Taiwan

(Received 17 May 2010; published 1 October 2010)

We theoretically verify that converting the Hermite-Gaussian modes into the Laguerre-Gaussian can lead to the spatial morphologies of the two-dimensional (2D) coherent states to be transformed from Lissajous figures to trochoidal curves. With this transformational relationship, we experimentally generate various structured light beams by exploiting a cylindrical-lens mode converter to transform the optical Lissajous modes. The present investigation manifests a notable method to generate optical coherent waves with various orbital spatial morphologies.

DOI: [10.1103/PhysRevA.82.043801](https://doi.org/10.1103/PhysRevA.82.043801)

PACS number(s): 42.50.Tx, 42.60.Jf, 03.65.Vf, 05.45.-a

I. INTRODUCTION

Numerous recent research on optical spatial modes has come out in modern physics [1–3] ranging from classical simulators of quantum entanglement [4–6] to parallel information [7,8]. The transverse Hermite-Gaussian (HG) modes are emitted by most laser cavities and are formally identical to the eigenstates of a two-dimensional (2D) quantum harmonic oscillator [9]. Consequently, HG modes are often used to represent the spatial quantum photon states within the paraxial regime [10]. Recently, a variety of quantum Lissajous states formed by the coherent superposition of HG eigenstates has been analogously generated from the degenerate laser resonators, which exhibit wave patterns resembling Lissajous figures [11]. Constructing wave states with spatial morphologies well localized on the particle orbits has become one of the most fundamental features in different branches of physics such as solid-state physics, nuclear and atomic physics, and laser physics [12,13].

Likewise, the Laguerre-Gaussian (LG) modes correspond to circular eigenstates of the 2D harmonic oscillator and play a prominent role in singular optics [14]. In the early 1990s, it was shown that a high-order HG mode can be converted into an LG mode by using astigmatic lenses [15,16]. Since this discovery, researchers have made tremendous progress in manipulation [17], detection [18], and application [19,20] of the orbital-angular-momentum states of light. The generation of optical coherent states with intensities localized on intriguing periodic orbits might be an enabling tool to explore further possibilities for creating a new class of quantum light-matter-entangled states.

In this work, we exploit the algebraic technique of quantum operators to explore the transformation of the spatial morphologies for the optical Lissajous states by converting their HG components into the corresponding LG modes. It is verified that the optical Lissajous states can be transformed into the optical trochoidal states with the spatial morphologies

corresponding to the trochoidal curves. We further employ the optical Lissajous modes and a $\pi/2$ -cylindrical-lens mode converter to realize the spatial transformation for generating optical trochoidal states. The present investigation manifests an intriguing nonclassical behavior of the coherent optical waves.

II. THEORETICAL ANALYSIS

The optical coherent wave is a superposition of degenerate laser modes and can provide a general description for a laser system exhibiting ray behavior. One aim of our work is to explore the spatial geometry of the optical coherent wave related to the HG and LG modes. The wave function of HG mode with longitudinal index n_3 and transverse indices n_1 and n_2 in Cartesian coordinates (x, y, z) is given by [9]

$$\Phi_{n_1, n_2, n_3}^{(HG)}(x, y, z) = \Phi_{n_1, n_2}^{(HG)}(x, y, z) e^{i(n_1 + n_2 + 1)\theta_G(z)} e^{-i\zeta_{n_1, n_2, n_3}(x, y, z)}, \quad (1)$$

where

$$\Phi_{n_1, n_2}^{(HG)}(x, y, z) = \frac{1}{\sqrt{2^{n_1 + n_2} \pi n_1! n_2!}} \frac{\sqrt{2}}{w(z)} H_{n_1} \left(\frac{\sqrt{2}x}{w(z)} \right) \times H_{n_2} \left(\frac{\sqrt{2}y}{w(z)} \right) \exp \left[-\frac{x^2 + y^2}{w(z)^2} \right], \quad (2)$$

where $w(z) = w_0 \sqrt{1 + (z/z_R)^2}$, $\zeta_{n_1, n_2, n_3}(x, y, z) = k_{n_1, n_2, n_3} z [1 + (x^2 + y^2)/2(z^2 + z_R^2)]$, w_0 is the beam radius at the waist, $z_R = \pi w_0^2/\lambda$ is the Rayleigh range, $H_n(\cdot)$ are the Hermite polynomials, k_{n_1, n_2, n_3} is the wave number, and $\theta_G(z) = \tan^{-1}(z/z_R)$ is the Gouy phase. In terms of the effective cavity length L , the wave number k_{n_1, n_2, n_3} is given by

$$k_{n_1, n_2, n_3} L = \pi [n_3 + (n_1 + n_2)(\Delta f_T/\Delta f_L)], \quad (3)$$

where $\Delta f_L = c/2L$ is the longitudinal mode spacing and Δf_T is the transverse mode spacing. When the ratio $\Delta f_T/\Delta f_L$ is close to a simple fractional, it has been shown that the longitudinal-transverse coupling usually leads to the frequency locking among different transverse modes with the help of different longitudinal orders [11]. Consequently, when the

*Correspondence: Dr. Yung-Fu Chen, Department of Electrophysics, National Chiao Tung University, 1001 TA Hsueh Road, Hsinchu, Taiwan 30050; E-mail: yfchen@cc.nctu.edu.tw

mode-spacing ratio $\Delta f_T/\Delta f_L$ is locked to a rational number P/Q , the group of the HG modes $\Phi_{n_1+pk, n_2+qk, n_3+sk}^{(HG)}$ with $k = \dots, -2, -1, 0, 1, 2, \dots$ can be found to constitute a family of frequency degenerate states, provided that the given integers (p, q, s) obey the equation $s + (p \mp q)(P/Q) = 0$. For convenience, the integers p and q are taken to be positive. The equation $s + (p \mp q)(P/Q) = 0$ indicates that $p \mp q$ needs to be an integral multiple of Q , i.e., $p \mp q = KQ$, where K is an integer.

With the coherent-state representation [11], the optical coherent wave formed by the family of the degenerated HG modes $\Phi_{n_1+pk, n_2+qk, n_3+sk}^{(HG)}$ can be expressed as

$$|\Psi_{\bar{n}_1, \bar{n}_2, \bar{n}_3}^{\pm p, q, s}(\gamma)\rangle = \sum_{k=-M}^M C_{M,k} e^{ik\gamma} |\Phi_{\bar{n}_1+pk, \bar{n}_2+qk, \bar{n}_3+sk}^{(HG)}\rangle, \quad (4)$$

where

$$C_{M,k} = 2^{-M} \binom{2M}{M+k}^{-1/2}$$

is the weighting coefficient,

$$\binom{n}{k} = \frac{n!}{k!(n-k)!}$$

represents the binomial coefficient, the parameter $\gamma = p\phi_1 \mp q\phi_2$ is the relative phase between various HG modes at $z = 0$, ϕ_1 and ϕ_2 are the phase factors related to the wave pattern, and \bar{n}_1, \bar{n}_2 , and \bar{n}_3 are the mean orders. With the expression of Eq. (1), the HG coherent wave can be expressed as

$$|\Psi_{\bar{n}_1, \bar{n}_2, \bar{n}_3}^{\pm p, q, s}(\gamma)\rangle = |\Psi_{\bar{n}_1, \bar{n}_2}^{\pm p, q}(\gamma)\rangle e^{i(\bar{n}_1+\bar{n}_2+1)\theta_G(z)} e^{-i\zeta_{\bar{n}_1, \bar{n}_2, \bar{n}_3}(x, y, z)} \quad (5)$$

with

$$|\Psi_{\bar{n}_1, \bar{n}_2}^{\pm p, q}(\gamma)\rangle = \sum_{k=-M}^M C_{M,k} e^{ik(p\mp q)\theta_G(z)} e^{ik\gamma} |\Phi_{\bar{n}_1+pk, \bar{n}_2+qk}^{(HG)}\rangle. \quad (6)$$

The wave pattern of the coherent state $|\Psi_{\bar{n}_1, \bar{n}_2}^{\pm p, q}(\gamma)\rangle$ has been shown to be localized on the Lissajous parametric surface: $x(\vartheta, z) = \text{Re}[X(\vartheta, z)]$; $y(\vartheta, z) = \text{Re}[Y(\vartheta, z)]$, where $X(\vartheta, z) = \sqrt{\bar{n}_1}w(z)e^{i[q\vartheta - \theta_G(z) - \phi_1]}$, $Y(\vartheta, z) = \sqrt{\bar{n}_2}w(z)e^{i[\pm p\vartheta - \theta_G(z) - \phi_2]}$, $0 \leq \vartheta \leq 2\pi$ and $-\infty \leq z \leq \infty$. Explicitly, the Lissajous parametric surface is formed by the Lissajous curves with the phase factor varying with the position z . Note that these Lissajous orbits are invariant with respect to changes in the phases ϕ_1 and ϕ_2 , provided that the quantity $\gamma = p\phi_1 \mp q\phi_2$ is conserved modulo 2π .

It had been experimentally realized in optics that an HG mode could be transformed with cylindrical lenses into an LG mode. As discussed above, the coherent states formed by the HG modes represent the quantum Lissajous states that display the spatial morphologies concentrating on the Lissajous figures. It is intriguing to explore the change of the spatial morphology for a Lissajous coherent state passing through cylindrical lenses that transforms each HG component into the corresponding LG mode. Replacing the HG modes with the corresponding LG modes in Eq. (6), the coherent state formed by LG modes is given by

$$|\Theta_{\bar{n}_1, \bar{n}_2}^{\pm p, q}(\gamma)\rangle = \sum_{k=-M}^M C_{M,k} e^{ik(p\mp q)\theta_G(z)} e^{ik\gamma} |\Phi_{\bar{n}_1+pk, \bar{n}_2+qk}^{(LG)}\rangle. \quad (7)$$

Since the Hermite-Gaussian modes of the laser resonator are isomorphic to the eigenstates of the 2D quantum harmonic oscillator, we can use the quantum operator algebra of the harmonic oscillator to deduce the subtle relationship between the Hermite-Gaussian and Laguerre-Gaussian coherent states. With the algebra of the ladder operators, the relationship between the LG and HG modes can be given by

$$|\Phi_{n_1, n_2}^{(LG)}\rangle = \hat{U} |\Phi_{n_1, n_2}^{(HG)}\rangle = \sum_{m_1=0}^N (i)^{m_1} d_{m_1 - \frac{N}{2}, n_1 - \frac{N}{2}}^{\frac{N}{2}} \left(\frac{\pi}{2}\right) |\Phi_{m_1, m_2}^{(HG)}\rangle, \quad (8)$$

where $N = n_1 + n_2 = m_1 + m_2$ and

$$d_{m_1 - \frac{N}{2}, n_1 - \frac{N}{2}}^{\frac{N}{2}}(\beta) = \sqrt{m_1!(N-m_1)!n_1!(N-n_1)!} \sum_{v=\max[0, m_1 - n_1]}^{\min[N-n_1, m_1]} (-1)^v [\cos(\beta/2)]^{N-n_1+m_1-2v} [\sin(\beta/2)]^{n_1-m_1+2v} \times \frac{1}{v!(N-n_1-v)!(m_1-v)!(n_1-m_1+v)!}. \quad (9)$$

Using the correspondence between classical canonical transform and quantum unitary transform [13] and the isomorphic relation between SU(2) algebra and SO(3) algebra, the LG coherent state $|\Theta_{\bar{n}_1, \bar{n}_2}^{\pm p, q}(\gamma)\rangle$ can be verified to be exactly localized on the parametric surface: $x(\vartheta, z) = \text{Re}[\tilde{X}(\vartheta, z)]$; $y(\vartheta, z) = \text{Re}[\tilde{Y}(\vartheta, z)]$, where $\tilde{X}(\vartheta, z) = (1/\sqrt{2})[X(\vartheta, z) - Y(\vartheta, z)]$, $\tilde{Y}(\vartheta, z) = (i/\sqrt{2})[X(\vartheta, z) + Y(\vartheta, z)]$, $0 \leq \vartheta \leq 2\pi$, and $-\infty \leq z \leq \infty$. Consequently, the spatial morphologies of the LG coherent states $|\Theta_{\bar{n}_1, \bar{n}_2}^{\pm p, q}(\gamma)\rangle$ correspond to the trochoidal orbits:

$$x(\vartheta, z) = w(z) \{ \sqrt{\bar{n}_1} \cos[q\vartheta - \theta_G(z) - \phi_1] - \sqrt{\bar{n}_2} \cos[\pm p\vartheta - \theta_G(z) - \phi_2] \} \quad (10a)$$

$$y(\vartheta, z) = w(z) \{ \sqrt{\bar{n}_1} \sin[q\vartheta - \theta_G(z) - \phi_1] + \sqrt{\bar{n}_2} \sin[\pm p\vartheta - \theta_G(z) - \phi_2] \}. \quad (10b)$$

Intriguingly, changing the eigenstate components in the coherent state from the HG modes $|\Phi_{n_1, n_2}^{(HG)}\rangle$ to the LG modes $|\Phi_{n_1, n_2}^{(LG)}\rangle$ can bring about the corresponding orbits to transform from Lissajous figures to trochoidal curves. This transformational relationship indicates that the stationary Lissajous state $|\Psi_{\bar{n}_1, \bar{n}_2}^{\pm p, q}(\gamma)\rangle$ in Eq. (6) can be converted into a stationary trochoid state with cylindrical lenses. Note that the trochoidal orbit in Eq. (10) can be found to be a hypotrochoid or an epitrochoid, depending on the sign \pm in the LG coherent states $|\Theta_{\bar{n}_1, \bar{n}_2}^{\pm p, q}(\gamma)\rangle$.

III. EXPERIMENTAL REALIZATION

The stationary Lissajous states $|\Psi_{\bar{n}_1, \bar{n}_2}^{\pm p, q}(\gamma)\rangle$ have been analogously generated from various degenerate laser cavities for several hundred different (p, q) [11]. Here we employ the laser modes associated with stationary Lissajous states to realize the transformational relationship between optical Lissajous states and optical trochoid states. Figure 1 depicts the experimental setup for transforming the Lissajous laser modes into the trochoid laser modes with cylindrical lenses. The present

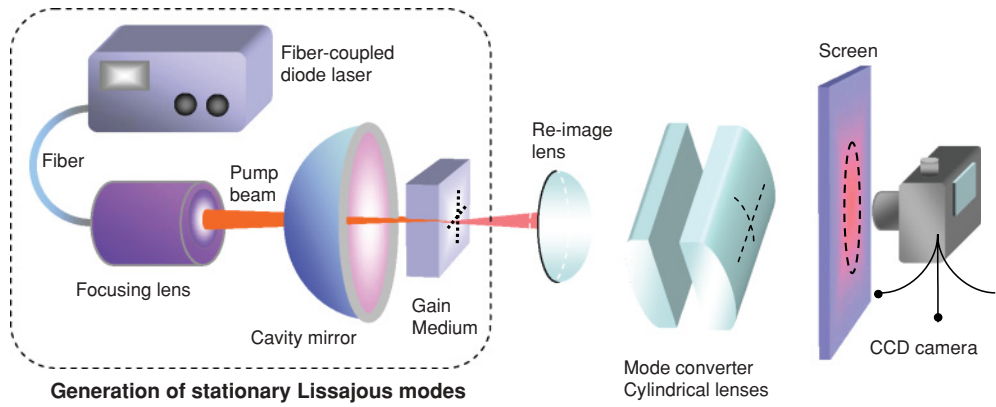


FIG. 1. (Color online) Experimental setup for transforming the Lissajous laser modes into the trochoid laser modes with cylindrical lenses.

laser cavity was composed of a spherical mirror and a large-aperture gain medium. The spherical mirror was a 10-mm radius-of-curvature concave mirror with antireflection coating at the pumping wavelength on the entrance face ($R < 0.2\%$), high-reflection coating at lasing wavelength ($R > 99.8\%$), and high-transmission coating at the pumping wavelength on the other surface ($T > 95\%$). The gain medium was an a -cut 2.0 at.% Nd:YVO₄ crystal with the length of 2 mm and the cross section of $8 \times 8 \text{ mm}^2$. One planar surface of the laser crystal was coated for antireflection at the pumping and lasing wavelengths; the other surface was coated to be an output coupler with the reflectivity of 99%. The pump source was a 2-W 809-nm fiber-coupled laser diode with a core diameter of $100 \mu\text{m}$. A coupling lens was used to focus the pump beam into the laser crystal with a large off-axis displacement. It has been found that the longitudinal-transverse coupling and the mode-locking effect in large-Fresnel-number spherical laser cavities usually drive the laser modes to be the coherent waves

that are transversely localized on the Lissajous figures with the relative phase continuously varying with the longitudinal direction. The generated Lissajous laser mode was reimaged into a cylindrical-lens mode converter to perform the beam transformation. The focal length of the cylindrical lenses was $f = 25 \text{ mm}$; the distance was precisely adjusted to be $\sqrt{2}f$ for the operation of the $\pi/2$ converter. To image the transformed transverse pattern, the transformed laser beam was directly projected on a paper screen at a distance of $\sim 50 \text{ cm}$ behind the cylindrical mode converter and the scattered light was captured by a digital camera.

Figures 2(a)–2(e) and Figs. 2(a')–2(e') show the experimental results for the input Lissajous laser modes $|\Psi_{\vec{n}_1, \vec{n}_2}^{\pm p, q}(\gamma)\rangle$ with the positive sign and the corresponding output laser modes converted from cylindrical lenses, respectively. The spatial morphologies of the laser modes can be clear seen to be transformed from Lissajous figures to hypotrochoidal curves. The related orbits for the transformed laser modes

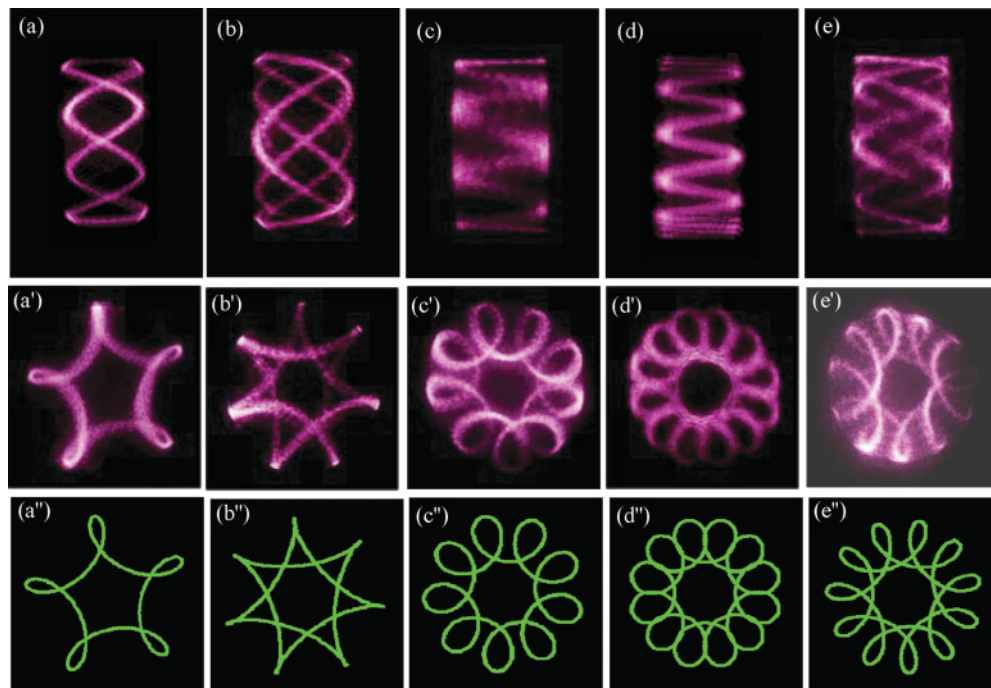


FIG. 2. (Color online) [(a)–(e)] Input Lissajous laser modes. [(a')–(e')] Output hypotrochoidal laser modes. [(a'')–(e'')] Related periodic orbits calculated with Eq.(13). For detailed descriptions for the parameters, see the text.

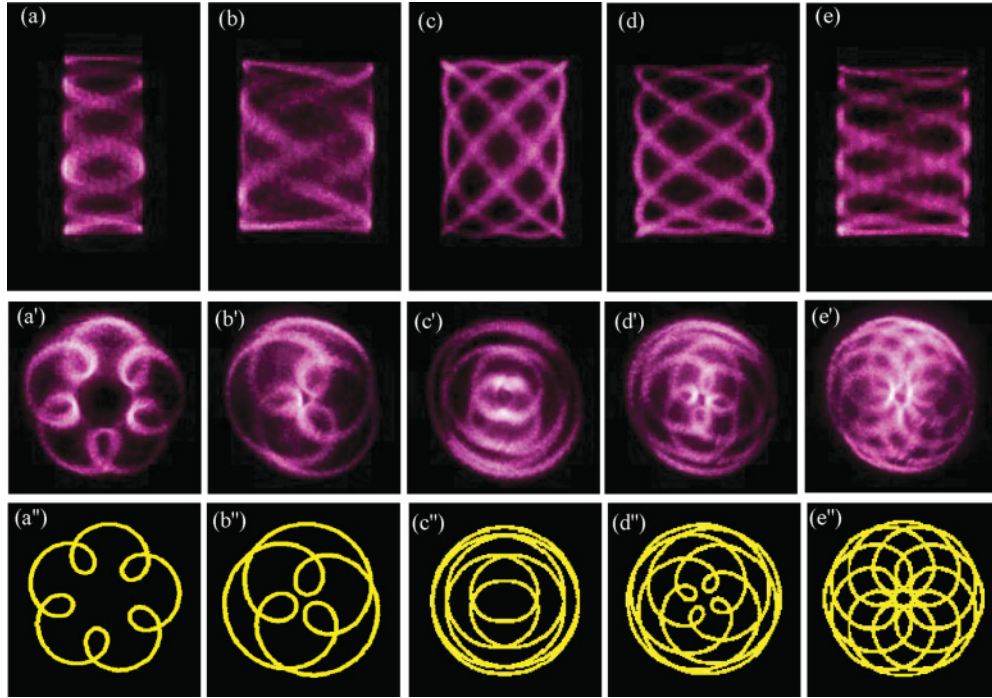


FIG. 3. (Color online) [(a)–(e)] Input Lissajous laser modes. [(a')–(e')] Output epitrochoidal laser modes. [(a'')–(e'')] Related periodic orbits calculated with Eq.(13). For detailed descriptions for the parameters, see the text.

can be calculated with Eq. (10) and are illustrated in Figs. 2(a'')–2(e''). The parameters for fitting to the experimental results are $(p, q) = (1, 4)$, $(\bar{n}_1, \bar{n}_2) = (45, 245)$, $(\phi_1, \phi_2) = (\pi/2, 0)$ for Fig. 2(a''); $(p, q) = (2, 5)$, $(\bar{n}_1, \bar{n}_2) = (40, 219)$, $(\phi_1, \phi_2) = (\pi/4, 0)$ for Fig. 2(b''); $(p, q) = (1, 8)$, $(\bar{n}_1, \bar{n}_2) = (45, 318)$, $(\phi_1, \phi_2) = (0, 0)$ for Fig. 2(c''); $(p, q) = (1, 11)$, $(\bar{n}_1, \bar{n}_2) = (42, 229)$, $(\phi_1, \phi_2) = (0, 0)$ for Fig. 2(d''); $(p, q) = (2, 9)$, $(\bar{n}_1, \bar{n}_2) = (50, 272)$, $(\phi_1, \phi_2) = (\pi/4, 0)$ for Fig. 2(e''). Experimentally, the parameters (p, q) are changed according to different cavity length, and (\bar{n}_1, \bar{n}_2) are estimated for varying degree of off-axis pumping. The phase factor (ϕ_1, ϕ_2) , related to the initial conditions of the coherent waves, is dominated by the laser cavity for minimum mode radius.

Figures 3(a)–3(e) and Figs. 3(a'')–3(e'') show the experimental results for the input Lissajous laser modes $|\Psi_{\bar{n}_1, \bar{n}_2}^{\pm p, q}(\gamma)\rangle$ with negative sign and the corresponding output laser modes converted from cylindrical lenses, respectively. Instead of hypotrochoids, the spatial morphologies of the laser modes are transformed from Lissajous figures to epitrochoidal curves due to the negative sign of ω_1/ω_2 . Figures 3(a'')–3(e'') depict the corresponding orbits calculated with Eq. (10). The parameters for fitting to the experimental results are $(p, q) = (1, 6)$, $(\bar{n}_1, \bar{n}_2) = (44, 240)$, $(\phi_1, \phi_2) = (\pi/2, 0)$ for Fig. 3(a''); $(p, q) = (2, 5)$, $(\bar{n}_1, \bar{n}_2) = (125, 180)$, $(\phi_1, \phi_2) = (\pi/4, 0)$ for Fig. 3(b''); $(p, q) = (6, 8)$, $(\bar{n}_1, \bar{n}_2) = (80, 245)$, $(\phi_1, \phi_2) = (0, 0)$ for Fig. 3(c''); $(p, q) = (5, 9)$, $(\bar{n}_1, \bar{n}_2) = (80, 125)$,

$(\phi_1, \phi_2) = (0, 0)$ for Fig. 3(d''); $(p, q) = (3, 11)$, $(\bar{n}_1, \bar{n}_2) = (160, 250)$, $(\phi_1, \phi_2) = (0, 0)$ for Fig. 3(e''). More importantly, the spatial morphologies of Lissajous states $|\Psi_{\bar{n}_1, \bar{n}_2}^{\pm p, q}(\gamma)\rangle$ are independent of the sign \pm ; however, the sign difference can be manifested from the spatial morphologies of the beams transformed by cylindrical lenses.

IV. CONCLUSIONS

In conclusion, we have verified that the spatial morphologies of the optical Lissajous states can be transformed into the optical trochoidal states with spatial morphologies corresponding to the trochoidal curves by converting the HG components into the corresponding LG modes. We have further exploited the optical Lissajous modes and a $\pi/2$ -cylindrical-lens mode converter to perform the spatial transformation in analogous way and to generate the optical trochoidal modes. Experimental realization confirmed a notable method to generate the spatial coherent states with various orbital morphologies. The present method is expected to be constructive for investigating the spatial transformation of optical coherent waves.

ACKNOWLEDGMENTS

This work is supported by the National Science Council of Taiwan (Contract No. NSC-97-2112-M-009-016-MY3).

- [1] D. Dragoman and M. Dragoman, *Prog. Quantum Electron.* **23**, 131 (1999).
 [2] D. Dragoman and M. Dragoman, *Quantum-Classical Analogies* (Springer, Berlin, 2004).

- [3] S. Longhi, *Laser & Photon. Rev.* **3**, 243 (2009).
 [4] K. Wagner *et al.*, *Science* **321**, 541 (2008).
 [5] J. Fu *et al.*, *Phys. Rev. A* **70**, 042313 (2004).
 [6] N. K. Langford *et al.*, *Phys. Rev. Lett.* **93**, 053601 (2004).

- [7] M. Lassen *et al.*, *Phys. Rev. Lett.* **98**, 083602 (2007).
- [8] G. F. Calvo and A. Picón, *Phys. Rev. A* **77**, 012302 (2008).
- [9] G. Nienhuis and L. Allen, *Phys. Rev. A* **48**, 656 (1993).
- [10] G. F. Calvo, A. Picón, and R. Zambrini, *Phys. Rev. Lett.* **100**, 173902 (2008).
- [11] Y. F. Chen *et al.*, *Phys. Rev. Lett.* **96**, 213902 (2006).
- [12] C. Lena, D. Delandé, and J. C. Gay, *Europhys. Lett.* **15**, 697 (1991).
- [13] T. H. Lu *et al.*, *Phys. Rev. Lett.* **101**, 233901 (2008).
- [14] M. S. Soskin and M. V. Vasnetsov, *Prog. Opt.* **42**, 219 (2001).
- [15] E. Abramochkin and V. Volostnikov, *Opt. Commun.* **83**, 123 (1991).
- [16] M. W. Beijersbergen *et al.*, *Opt. Commun.* **96**, 123 (1993).
- [17] D. Akamastu and M. Kozuma, *Phys. Rev. A* **67**, 023803 (2003).
- [18] J. Leach, M. J. Padgett, S. M. Barnett, S. Franke-Arnold, and J. Courtial, *Phys. Rev. Lett.* **88**, 257901 (2002).
- [19] H. He *et al.*, *Phys. Rev. Lett.* **75**, 826 (1995).
- [20] D. G. Grier, *Nature* **424**, 810 (2003).